IR Sensor-based Grasp Planner for the Pisa/IIT Softhand Under Uncertainty

E. Luberto, G. Santaera, Y. Wu, M. Gabiccini

***Abstract*— This paper presents an approach to refine grasps for soft robotic hands in the presence of uncertainty. Once a pre-planned grasp, e.g. from a database, has been selected for execution to an object detected in a scene, an infrared sensor-informed grasp planner is run that essentially reduces uncertainties related to object shape and its pose in the environment. The proposed method implements a grasp location optimization algorithm that allows to minimize the distances between hand fingertips and the object by continuously controlling the wrist pose and the amount of hand closing. Experimental studies with Kuka-lwr arm and Pisa/IIT Softhand illustrate the benefit of the developed technique and the improvement in the grasping performance with respect to the open-loop execution of grasps planned on the basis of prior visual cues only.**

I. INTRODUCTION

The problem of autonomous robotic grasping has been in the focus of robotic research community for the past several decades [1], [2], [3]. Intelligent, proficient grasp planners have been developed that allow robotic hand to perform grasping tasks closely to humans. For ideal scenarios, where the object shape and location are perfectly known, and precise control of robotic hand can be achieved, pre-programmed autonomous grasping may be possible. To this end, most of the proposed planners [4], [5] rely on finding optimal fingertip placement on the object, while the surrounding environments are considered to be avoided as obstacles. However, these approaches are limited by their hand rigidity and fragility, and the manipulation strategies are very far from those a human would execute in real scenarios.

A real-world grasps are often associated to some uncertainties, the most typical ones being related to object recognition and localization. Usually, robots are equipped with vision sensors [6], [7], [8] to help reducing this uncertainty. However, a certain amount of uncertainty is usually unavoidable due to poor vision results, or incomplete view coverage of the sensor, etc. Other uncertainty may correspond to unexpected location of the object, where in this case, tactile/torque sensors are required to gain some additional information and to refine the object location from contacts [9], [10], [11]. Therefore, dexterous grasping of objects under uncertainty remains a difficult and unsolved problem in robotics.

E. Luberto, G. Santaera, Y. Wu are with Centro di Ricerca E. Piaggio, Universit di Pisa, Largo L. Lazzarino 1, 56122 Pisa, Italy. santaeragaspare@inwind.it, ema.lbt@hotmail.it, yier.wu@for.unipi.it

M. Gabiccini is with Dipartimento di Ingegneria Civile e Industriale (DICI), Largo Lucio Lazzarino 1, 56122 Pisa, with Centro di Ricerca E. Piaggio, Universit di Pisa, Largo L. Lazzarino 1, 56122 Pisa, and with Department of Advanced Robotics (ADVR), Italian Institute of Technology, Via Morego 30, 16163 Genova, Italy. m.gabiccini@ing.unipi.it

Fig. 1. Pisa/IIT Softhand with IR Sensors

To better tackle the above described types of uncertainty, researchers have proposed the use of underactuated and/or soft hands [12], [13]. The design is simpler, easier to control and allows object contact with hand parts other than the fingertips, as well as to explore the surrounding environment in order to achieve precise and stable grasp. The robotic hand studied in this paper is the Pisa/IIT Softhand [14], which has only one degree of actuation, and is continuously deformable in an infinity of possible shapes through interaction with objects and environment. Incipient grasp with this type of Softhand has been successfully achieved with a wide variety of everyday objects [15]. However, problems still remain when one or several above mentioned uncertainties occur during the execution of grasping tasks with novel objects.

The lack of exact knowledge of target object shape and location in the environment can be compensated by the use of sensor feedback. To further improve the quality and reliability of robotic grasping, different strategies have been proposed to enhance the sensing capabilities of robotic manipulators. Enhancement of long-range vision sensor is one of the solutions, such as in-hand object tracking, hand extraction for object reconstruction, etc. However in general, image acquisition and processing are quite slow for online reactive response. Another solution relies on tactile sensors, which have been employed in numerous tasks [16], [17], whereas they require premature contacts with the object and may cause significant object motion.

On the other hand, short-range infrared (IR) sensors are widely used in robotic applications thanks to their low-cost, fast response time and reduced sensitivity to the environment. In robotic grasping, IR sensors have been introduced during

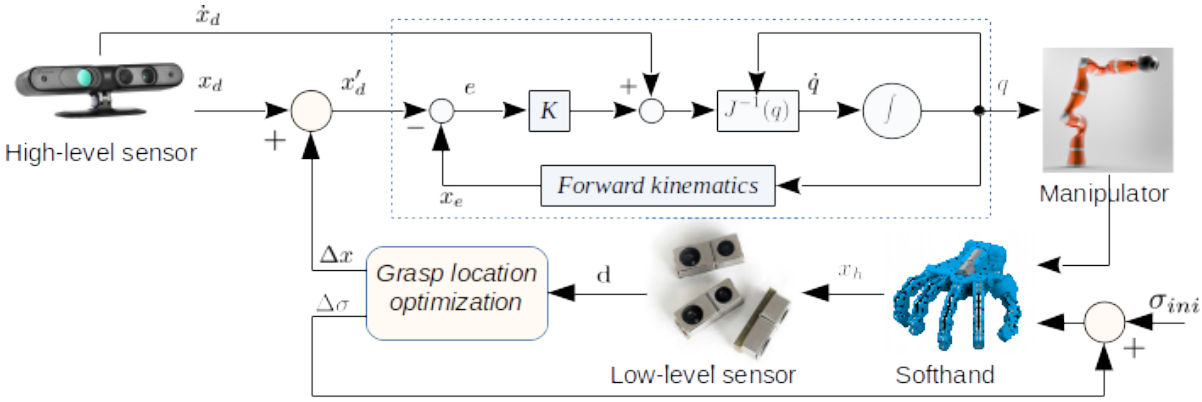

Fig. 2. Control Scheme of Sensor-based Grasping

final grasp adjustments. In [18], the authors detect the orientation of an object surface using the IR sensors that fit inside the fingers. In [19], a shared-control algorithm has been proposed based on long-range vision sensor and infrared sensors for teleoperation-based grasping. In [20], robust grasping has been achieved using an IR Net-structure proximity sensor for objects with unknown position and attitude. However, these approaches have been developed for robotic hands with sensible rigidity and high degrees of actuation (4-8). Limited number of work address the problem of grasping refinement for compliant hands based on IR sensor measurements, which looks very promising here.

In this work, an approach to grasp refinement for the Pisa/IIT Softhand under uncertainty using IR sensors is presented. Based on sensor measurement feedback, the proposed algorithm allows to center the Softhand fingers around the object and wrap the hand around it in a uniform manner. It is effective, high-speed, does not cause premature object contact nor needs re-grasping strategies. It allows the robotic hand to perform online adjustments before final grasping.

To address the above mentioned problems, the remainder of the paper is organized as follows. Section II presents the problem of grasping with our Softhand. Section III describes the IR sensor working principle and the measurements is provided. In Section IV, an algorithm of grasp location refinement of the Softhand is presented. Section V contains the experimental results obtained for IR sensor-based grasp of novel objects using Kuka-lwr and Pisa/IIT Softhand. Finally, Section VI summarizes the main results and contributions of this paper.

II. PROBLEM STATEMENT

Despite the fact that contemporary vision systems are able to reconstruct fairly good 3D object models, which allows to considerably reduce the related uncertainties, it requires enormous time and manpower to build a point cloud library for each novel object, yet still incomplete to guarantee a stable final grasp. To reduce the time of visual acquisition and processing, we propose to use only the prior visual cue of an object, which leads the robot to a so-called pre-grasp location. In order to ensure a stable final grasp, infrared sensors are mounted on the hand fingertips to gain some additional information about the hand location with respect to the object.

(a) Unexpected object location (b) Unexpected object motion

Fig. 3. Types of uncertainty during grasping

For the considered compliant hand, due to the peculiarities of its embedded soft and adaptive synergy [14], its configuration and exact fingertip locations are usually unknown after a grasp is executed. Therefore, the target object is approached by the hand via controlling wrist pose and hand closing. In order to improve the quality of grasp, we proposed to minimize the distances between hand fingertips by continuously controlling the wrist pose and the amount of hand closing based on IR sensor measurements. As the hand is closed in an informed manner, the proposed method allows to reduce the chance of significantly perturbing the object during the execution of the final grasp.

The overall control scheme of the robotic arm and hand is depicted in Fig. 2. The proposed grasp location optimization algorithm provides the correction values of wrist pose and hand closing at each time step. This control strategy allows to effectively improve the quality of grasp under uncertainty, such as visual incompletion and/or coverage, unexpected change of object location, etc. (see Fig. 3).

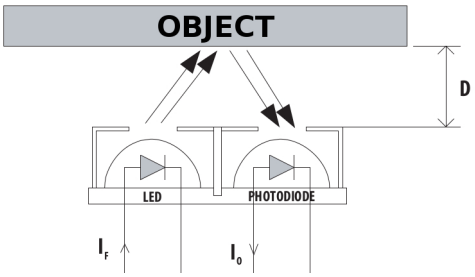

Fig. 4. IR Sensor working principle

III. SENSOR MEASUREMENTS

To measure the distances between hand fingertips and target object, we proposed to use infrared sensor. Its advantages include small size, low-cost, mechanical robustness and the simplicity to be managed with a micro-controller. The sensor consists of only one emitter and one receiver (See Fig. 4). The intensity of the transmitted infrared wave decreases according to the well known exponential law

$$E = E_0 e^{-\alpha x}, \tag{1}$$

where E_0 is the intensity of the original wave, x depends on the wave direction, and the parameter α varies with the material and increases with the wave frequency.

When the transmitted wave meets an object it splits in two, a refracted wave that spreads onto the object and a reflected one that comes back and meets the receiver. The intensity of these two waves depends on the reflection coefficient of the object material and on the angle at which the transmitted wave hits the object. The relation between the transmitted, refracted and reflected wave can be obtained using the Snell's law

$$k_1 \sin\theta_1 = k_2 \sin\theta_2, \tag{2}$$

where k_1, k_2 depend on the materials characteristics and θ_1, θ_2 are the angles between the wave travelling direction and the normal to the object surface. Usually the infrared wave is being transmitted and reflected through the same medium (the air, for instance), so $k_1 = k_2$ and, consequently, $\theta_1 = \theta_2$. Therefore, the desired distance between sensor and object can be obtained by measuring the intensities of the two waves.

However in most cases, it is hardly possible to know *a priori* the property of object material. To overcome this problem, one possible solution is to use the flight time, meaning that the sensor counts the time between the emission and reception of the infrared wave. Corresponding distance can be obtained as

$$d = \frac{v t_f}{2}, \tag{3}$$

where v is the wave propagation velocity, t_f is the flight time.

IV. GRASP REFINEMENT ALGORITHM

The IR sensors are mounted on the distal phalanges of all/a subset of the Softhand fingers, according to the sensors' visibility w.r.t the object. Fig. 1 shows one of the possible arrangements of IR sensors, where only the thumb, index and ring finger are equipped. The sensor readings provide the distances between the phalanges and object within a range of about 60mm. It is assumed that all sensor measurements are collected in a vector $\mathbf{d} = [d_1, d_2, ..., d_n]^T$, $d_i \geq 0$, where n indicates the number of sensors whose measurement is available (i.e. the sensor is seeing the object). Corresponding residual errors can be simply written as $r_i = d_i$. Since the goal is for the hand to approach the object in a homogeneous manner, the objective function of the optimization is defined as the root-mean-square errors of the residuals as follows

$$r_{ms} = \sqrt{\sum_{i=1}^{n} r_i^2} \tag{4}$$

The residual vector $\underline{\mathbf{r}} = [r_1, ...r_n]^T$ obtained from sensor measurements is in fact a function of control input parameters $\underline{\mathbf{x}}$, which are the decision variables of the grasp location optimization problem. The size and nature of $\underline{\mathbf{x}}$ vary with the parameters of the control input (e.g, for joint position control, $\underline{\mathbf{x}} = [j_1, ..., j_n]^T$, for wrist pose control, $\underline{\mathbf{x}} = [p_x, ..., p_z; r_x, ..., r_z]^T$). In this case, $\underline{\mathbf{x}}$ is defined by the arm wrist pose $(p_x, p_y, p_z; r_x, r_y, r_z)$ (6 DoF) together with the amount of hand closing, which is directly the synergy actuation (1 DoF), i.e. $\underline{\mathbf{x}} = [p_x, p_y, p_z; r_x, r_y, r_z; \sigma]^T$. The corresponding optimization problem can be formulated as

$$\min_{\underline{\mathbf{x}}} f(\underline{\mathbf{x}}), \quad \text{where} \quad f(\underline{\mathbf{x}}) = \frac{1}{2} \underline{\mathbf{r}}(\underline{\mathbf{x}})^T \underline{\mathbf{r}}(\underline{\mathbf{x}}) \tag{5}$$

which is a *nonlinear* quadratic function w.r.t the decision variables $\underline{\mathbf{x}}$.

It is worth noting that, in the experimental setting, $f(\underline{\mathbf{x}})$ is only computable through execution of moves and measurement of sensor outputs. To reconcile the use of a gradient-based optimization algorithm with the intrinsic numerical nature of our $f(\underline{\mathbf{x}})$, we employ a Gauss-Newton strategy and form a linear approximation of the residual as follows

$$\underline{\mathbf{r}}(\underline{\mathbf{x}}) \simeq \underline{\mathbf{r}}_L(\Delta\underline{\mathbf{x}}) = \underline{\mathbf{r}}(\underline{\mathbf{x}}_k) + \mathbf{J}_r(\underline{\mathbf{x}}_k) \cdot \Delta\underline{\mathbf{x}}, \text{ where } \mathbf{J}_r = \frac{\partial \underline{\mathbf{r}}}{\partial \underline{\mathbf{x}}} \tag{6}$$

such that the optimal solution can be found step by step via corrections of the control inputs such that $\underline{\mathbf{r}} \to 0$. In (6), $\underline{\mathbf{r}}(\underline{\mathbf{x}}_k)$ are the residuals measured at current step k, $\mathbf{J}_r$ is the Jacobian matrix of the residuals, and $\Delta\underline{\mathbf{x}}$ is the correction displacements, which represent the next move. Here, $\mathbf{J}_r$ is computed numerically based on the measurement data. In particular, each column can be expressed as

$$\mathbf{J}_r(:, j) = \frac{\delta \underline{\mathbf{r}}}{\delta \underline{\mathbf{x}}_j} \tag{7}$$

where $\delta\underline{\mathbf{r}}$ collects the changes in the measurements of residuals vector with respect to the change in each control

input $\delta\underline{\mathbf{x}}_j$. Using Eq. (5) and (6), one can obtain the solution of the quadratic approximation at step k

$$f_Q(\Delta\underline{\mathbf{x}}) = \frac{1}{2}\underline{\mathbf{r}}_L(\Delta\underline{\mathbf{x}})^T\,\underline{\mathbf{r}}_L(\Delta\underline{\mathbf{x}}) \tag{8}$$

of the original optimization problem (5) by seeking where $\left[\frac{\partial f_Q(\Delta\underline{\mathbf{x}}_k)}{\partial\Delta\underline{\mathbf{x}}_k}\right]^T = \underline{\mathbf{0}}$ which yields

$$\Delta\underline{\mathbf{x}}_k = -\mathbf{J}_r^+(\underline{\mathbf{x}}_k)\,\underline{\mathbf{r}}_k \tag{9}$$

Note that $\mathbf{J}_r^+ = \left(\mathbf{J}_r^T\mathbf{J}_r\right)^{-1}\mathbf{J}_r^T$ is the pseudo-inverse of the residual Jacobian. This allows us to update the succeeding hand location/configuration by adding the step

$$\underline{\mathbf{x}}_{k+1} = \underline{\mathbf{x}}_k + \alpha\Delta\underline{\mathbf{x}}_k \tag{10}$$

where $\alpha \in [0,1]$ is a scaling factor for tuning these steps.

Based on the above presented method for grasp location optimization, the corresponding algorithm considering a robotic arm with a grasping end-effector in general are summarized in Algorithm (1). It should be mentioned that the strategies for approaching and moving the end-effector in steps no. 4 and no. 5 seem ambiguous due to the fact that these strategies highly depends on the particular circumstance of the sensors arrangement and measurements. More details will be given in the section of experimental validation.

Algorithm 1: Grasp Location Optimization

1: Acquiring object information from a vision system and obtain the pre-grasp location for the robotic arm;
2: Moving the arm to the obtained location and bringing the grasping end-effector to a pre-grasp configuration;
3: Checking the sensor measurements:
if *All sensors have no measurements on the object* **then**
Goto Step no. 4;
if *At least one sensor has measurement on the object* **then**
Goto Step no. 5;
if *All sensors have measurements on the object* **then**
Goto Step no. 6;
4: Approaching the grasping end-effector to the object and returning to step no. 3;
5: Moving the grasping end-effector around the object according to particular strategy (depending on the sensors measurements), returning to step no. 3;
6: Moving the grasping end-effector by sequentially changing each parameter of the control input $\delta\underline{\mathbf{x}}$, while obtaining the differences in residual vector $\delta\underline{\mathbf{r}}$ based on sensor measurements and return the end-effector to its previous state;
7: Computing the residual Jacobian matrix using Eq. (7);
8: Computing the corrections $\Delta\underline{\mathbf{x}}$ for the succeeding step using Eq.(9);
9: Moving and Closing the grasping end-effector following Eq. (10), and reading the IR sensor measurements;
10: Computing the objective function r_{ms} using the new measurements:
if $r_{ms} >$ threshold **then**
Goto Step no. 6;
else
Grasp the Object!

V. EXPERIMENTAL VALIDATION

To confirm the applicability of the proposed grasp refinement algorithm and demonstrate its benefits from a piratical point of view, this section presents the experimental setup and procedure, the sensor particularity as well as the experiment results of grasping performances on a set of everyday objects.

A. Experiment setup and procedure

To perform the grasping tasked, the experiment setup includes the following units:

- A RGB-D sensor, Asus Xtion Prolive [21], for acquisition of the object image (in our case the frontal view only);
- A 7-dof robotic manipulator, Kuka Lightweight IV [22], for object manipulation (maxim payload 7kg);
- A 19-dof robotic hand, Pisa/IIT Softhand, for object grasping (one-dof actuation);
- Three short-range IR sensors, Avago HDSL9100, mounted on hand fingers for distance measurements;
- A experiment table and a set of selected everyday objects.

The grasp experiments are designed for two different case scenarios assuming the vision sensor captures the object frontal view only: (i) normal grasp; (ii) unexpected object locations. In case (i), all objects are assumed to be grasped at their predefined positions on the table. For objects have non-symmetrical form, grasping experiments are performed in two different object orientations. For each object and each object orientation, experiments are repeated for three times. In case (ii), the grasping experiments are performed where objects are slightly moved away from their predefined positions (in translations and/or in orientation, depending on the symmetricity of corresponding object form).

For comparison, grasping experiments are carried out both with and without applying the IR sensor-based optimization algorithm proposed in this paper. To demonstrate the advantages of the this method, the grasping performance analysis are given in the following subsections, in terms of successful rate of the grasp, evolution of measured distances and of the wrist poses.

B. Sensor particularity

In this work, the Avago HDSL9100 Infrared Sensor [23] (see Fig. 5) is selected thanks to its small size (7x3x2.5 mm), which allows it to be fit into the fingertips of Pisa/IIT Softhand, yet provides a suitable operative range (4-65 mm)

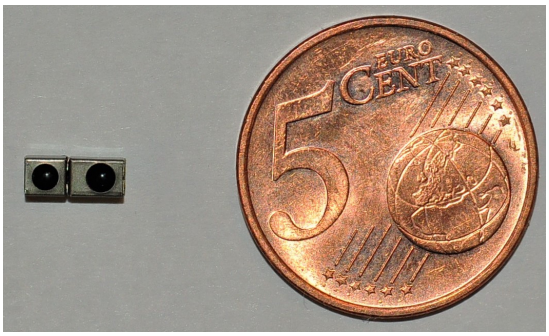

Fig. 5. Avago HDSL9100 Infrared Sensors

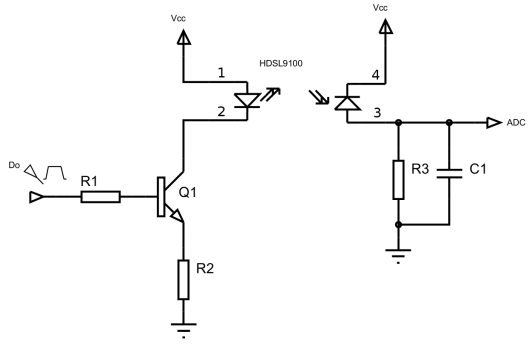

Fig. 6. Conditioning Circuit Schematic of IR Sensors

for the distance measurements. However due to the small size of the IR sensor, a conditioning circuit is required to manage the sensor input/output. It should be noted that the sensor operative range depends on the circuit components, here, they are tuned to obtain the maximum distance.

Another issue relates to closeness of the sensors due to their placements on the soft hand. In our experiment, three IR sensors are used and are mounted on the thumb, index and ring fingers (see Fig. 1). This arrangement may cause some disturbances during the measurements, for instance, the light emitted by one sensor could be misread by another. To overcome this problem, the conditioning circuit is designed to activate only one sensor at a time.

The schematic of conditioning circuit is illustrated in Fig. 6, where each sensor is activated by an square wave (*Do*), and its output is read by an analog-digital converter (*ADC*). The physical output of the sensor is an electric voltage, which is proportional to the intensity of the reflected wave in the receiver. In other words, the higher is the output voltage, the closer is the sensor to an object. The ADC returns the output voltage in a digital value in bits (or ticks), according to its resolution (12 bits on 5 Volt for the embedded micro-controller PSoC).

To simplify the design of conditioning circuit, instead of counting the sensor flight time (see Section III), we use directly the output value of the ADC. In fact, the proposed algorithm, step by step in a differential way, works to reduce the distances between the object and the robot end-effector. In each step it moves the end-effector of the robot and measures the distances, to understand which movements reduce these ones, so it does not need to know the exact value of distances in millimeters but considering the proportionality between distances and the intensities of the reflected waves, so the output value of the analog-digital converter is enough. Summing up this design choice allows to reduce the complexity of the conditioning circuit.

C. Checking the sensor measurements

In the Algorithm (1), before to compute the residual Jacobian matrix, one has to assure that all sensors are in the operative range. The check on the IR sensors, Step no. 3, depends on the specific configuration of the sensors installed. If at least one sensors measures a distance higher than 60 mm the current SoftHand position is changed. This displacement allows to explore the scenario exploiting the following criteria

- **case 1:** *(IRthumb)* $>$ th
  SH_x -= ρ
  SH_y += ρ
- **case 2:** *(IRindex)* $>$ th
  SH_x -= ρ
  SH_y -= ρ
  hand-closure += υ
- **case 3:** *(IRring)* $>$ th
  SH_x += ρ
  SH_y -= ρ
- **case 4:** *(IRthumb & IRindex)* $>$ th
  SH_x -= ρ
  SH_y -= ρ
- **case 5:** *(IRthumb & IRring)* $>$ th
  hand-closure += υ
- **case 6:** *(IRindex & IRring)* $>$ th
  SH_y -= ρ
- **case 7:** *(IRthumb & IRring & IRring)* $>$ th
  SH_x -= ρ
  SH_y -= ρ

where SH_x and SH_y are the position of the SoftHand frame in the world frame (see Fig. 7). ρ and υ represent the correction about position [mm] and hand-closure [tic], while th is setted on 60mm.

D. Grasp results

The overall grasping performance of all conducted experiments are given in Table I, where the number of successful grasps are provided for each object in each case. Comparison are made for grasping with and without the proposed algorithm.

Clearly, using only the object frontal view and performing the grasp task at corresponding pre-grasp location, the number of successful grasps is very low. In the second case scenario, when the objects are deliberately moved, the successful grasp reduced to none. Applying the proposed

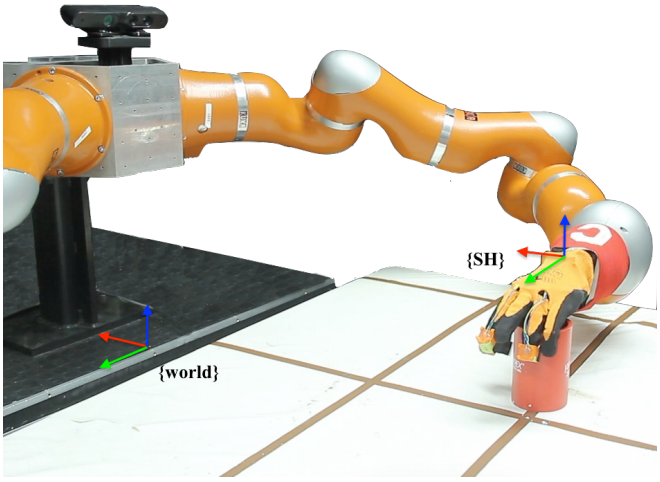

Fig. 7. Scenario

	Case (i)		Case (ii)	
Object	Algo.+	Algo.-	Algo.+	Algo.-
Cylinder	2/3	0	3	0
Baby cup	4	1	3	0
Paper box	4	1	2	0
Total	10	2	8	0

TABLE I

OVERALL GRASPING PERFORMANCE: SUCCESSFUL GRASP

grasp location optimization, the successful rate have been considerably increased by 54% and 53% in case (i) and (ii), respectively.

To evaluate the grasp results with applying the proposed sensor-based technique, the sensor measurements during the grasp have been analyzed. Fig. 8 and 9 illustrate the evolution of the measured distances between hand fingertips and objects for case scenario (i) and (ii), respectively. In particular, the blue dot line relates to the norm of all distances; the red star line shows the norm of corresponding residuals; and the markers are the distances from each fingertips to the object at each step.

In most of the performed grasp tasks, measurements of the index show that it is always further from the object then the others, whereas the thumb and ring are well centralized with respect to the object. This is due to the particular soft hand synergy, each finger closes differently driven by the hand closure. In this case, the index has relatively small amount of closure comparing to the other two fingers. However in practical grasp, such hand configuration can guarantee a stable grasp for most objects.

Table II and III present the sensor measurements before and after applying the grasp location optimization, for case scenarios (i) and (ii), respectively. The 3^{rd} column reports the hand distance to the object, the 4^{th} shows the residual values of all fingertips, and the last column considers only the thumb and ring. From these tables, it is clearly that

Object	Algo.	$\|\mathbf{d}\|$ (m)	$\|\mathbf{r}\|$ (m)	$\|\mathbf{r}^*\|$ (m)
Cylinder	Before	0.124	0.045	0.012
	After	0.037	0.020	0.002
Baby cup	Before	0.142	0.039	0.011
	After	0.034	0.017	0.001
Paper box	Before	0.094	0.040	0.013
	After	0.037	0.020	0.001

TABLE II

EVOLUTION OF DISTANCES AND RESIDUALS IN CASE (I)

Object	Algo.	$\|\mathbf{d}\|$	$\|\mathbf{r}\|$	$\|\mathbf{r}^*\|$
Cylinder	Before	0.119	0.021	0.010
	After	0.028	0.019	0.012
Baby cup	Before	0.139	0.018	0.004
	After	0.028	0.021	0.007
Paper box	Before	0.086	0.056	0.041
	After	0.025	0.010	0.003

TABLE III

EVOLUTION OF DISTANCES AND RESIDUALS IN CASE (II)

the proposed technique essentially reduced the distances from the hand to the object comparing to a pre-grasp configuration, and precisely centralized the thumb and ring around the object.

VI. CONCLUSIONS

In this paper we described an effective, high-speed method to refine the final grasping location, using low-cost IR sensors and optimization technique. The presented algorithm allows to center a robotic end-effector around an object, whose location and shape are acquired by a prior visual cue only. The algorithm was tested on Kuka-lwr arm and Pisa/IIT Softhand by performing grasp tasks under different uncertainties with a set of daily objects. The grasp experiments validates the effectiveness of the proposed method and showed essential improvement in the grasping performance. Future work will address the full use of the IR sensors on all fingers, taking into account the adaptive synergy of the softhand, to exploit the capabilities of the sensorized softhand for perception of unstructured environments.

VII. ACKNOWLEDGMENTS

This work is supported by the grant no. 600918 PACMAN - Probabilistic and Compositional Representations of Object for Robotic Manipulation - within the FP7-ICT- 2011-9, and under grant agreement no. 645599 ”SoMa” - Soft-bodied intelligence for Manipulation, within the H2020-ICT-2014-1.

REFERENCES

[1] A. Bicchi and V. Kumar, “Robotic grasping and contact: a review,” in *Robotics and Automation, 2000. Proceedings. ICRA ’00. IEEE International Conference on*, vol. 1, 2000, pp. 348–353.

[2] A. M. Okamura, N. Smaby, and M. R. Cutkosky, “An overview of dexterous manipulation,” in *Robotics and Automation, 2000. Proceedings. ICRA’00. IEEE International Conference on*, vol. 1. IEEE, 2000, pp. 255–262.

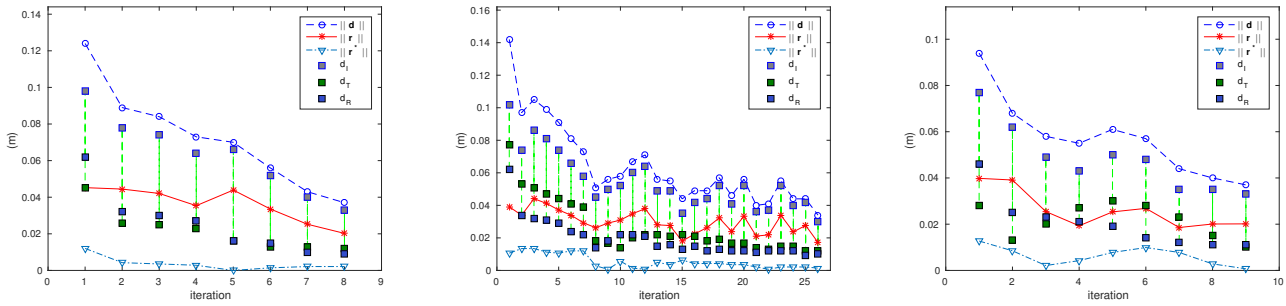

(a) Cylinder (b) Baby cup (c) Paper box

Fig. 8. Sensor measurements in case scenario (i)

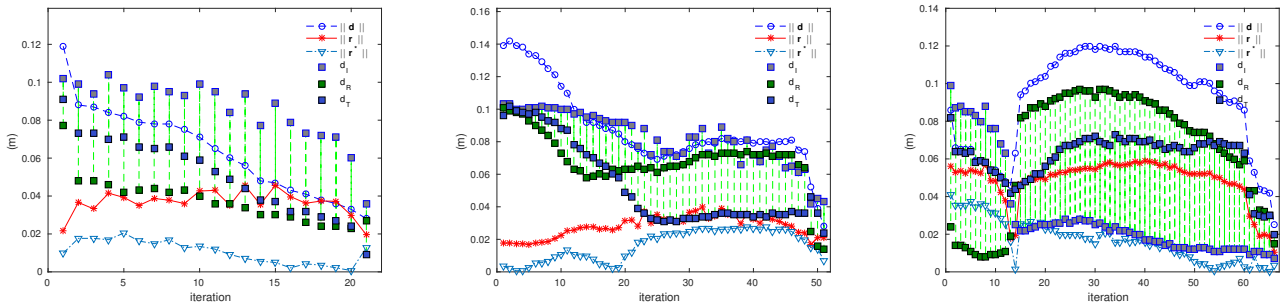

(a) Cylinder (b) Baby cup (c) Paper box

Fig. 9. Sensor measurements in case scenario (ii)

[3] C. C. Kemp, A. Edsinger, and E. Torres-Jara, "Challenges for robot manipulation in human environments," *IEEE Robotics and Automation Magazine*, vol. 14, no. 1, p. 20, 2007.

[4] R. Diankov and J. Kuffner, "Openrave: A planning architecture for autonomous robotics," *Robotics Institute, Pittsburgh, PA, Tech. Rep. CMU-RI-TR-08-34*, vol. 79, 2008.

[5] A. Miller and P. Allen, "Graspit! a versatile simulator for robotic grasping," *Robotics Automation Magazine, IEEE*, vol. 11, no. 4, pp. 110–122, 2004.

[6] C. Kemp, C. Anderson, H. Nguyen, A. Trevor, and Z. Xu, "A point-and-click interface for the real world: Laser designation of objects for mobile manipulation," in *Human-Robot Interaction (HRI), 2008 3rd ACM/IEEE International Conference on*, Mar. 2008, pp. 241–248.

[7] A. Saxena, J. Driemeyer, and A. Y. Ng, "Robotic grasping of novel objects using vision," *The International Journal of Robotics Research*, vol. 27, no. 2, pp. 157–173, 2008.

[8] B. Wang, L. Jiang, J. Li, and H. Cai, "Grasping unknown objects based on 3d model reconstruction," in *Advanced Intelligent Mechatronics. Proceedings, 2005 IEEE/ASME International Conference on*, Jul. 2005, pp. 461–466.

[9] J. Tegin and J. Wikander, "Tactile sensing in intelligent robotic manipulation-a review," *Industrial Robot: An International Journal*, vol. 32, no. 1, pp. 64–70, 2005.

[10] L. Natale and E. Torres-Jara, "A sensitive approach to grasping," in *Proceedings of the sixth international workshop on epigenetic robotics*. Citeseer, 2006, pp. 87–94.

[11] J. Romano, K. Hsiao, G. Niemeyer, S. Chitta, and K. Kuchenbecker, "Human-inspired robotic grasp control with tactile sensing," *Robotics, IEEE Transactions on*, vol. 27, no. 6, pp. 1067–1079, Dec. 2011.

[12] L. U. Odhner, L. P. Jentoft, M. R. Claffee, N. Corson, Y. Tenzer, R. R. Ma, M. Buehler, R. Kohout, R. D. Howe, and A. M. Dollar, "A compliant, underactuated hand for robust manipulation," *The International Journal of Robotics Research*, vol. 33, no. 5, pp. 736–752, 2014.

[13] R. Deimel and O. Brock, "A novel type of compliant and underactuated robotic hand for dexterous grasping," *The International Journal of Robotics Research*, p. 0278364915592961, 2015.

[14] M. G. Catalano, G. Grioli, E. Farnioli, A. Serio, C. Piazza, and A. Bicchi, "Adaptive synergies for the design and control of the pisa/iit softhand," *The International Journal of Robotics Research*, vol. 33, no. 5, pp. 768–782, 2014.

[15] M. Bonilla, E. Farnioli, C. Piazza, M. Catalano, G. Grioli, M. Garabini, M. Gabiccini, and A. Bicchi, "Grasping with soft hands," in *Humanoid Robots (Humanoids), 2014 14th IEEE-RAS International Conference on*. IEEE, 2014, pp. 581–587.

[16] D. Gunji, Y. Mizoguchi, S. Teshigawara, A. Ming, A. Namiki, M. Ishikawaand, and M. Shimojo, "Grasping force control of multi-fingered robot hand based on slip detection using tactile sensor," in *Robotics and Automation, 2008. ICRA 2008. IEEE International Conference on*, May 2008, pp. 2605–2610.

[17] J. Felip and A. Morales, "Robust sensor-based grasp primitive for a three-finger robot hand," in *Intelligent Robots and Systems, 2009. IROS 2009. IEEE/RSJ International Conference on*. IEEE, 2009, pp. 1811–1816.

[18] K. Hsiao, P. Nangeroni, M. Huber, A. Saxena, and A. Ng, "Reactive grasping using optical proximity sensors," in *Robotics and Automation, 2009. ICRA '09. IEEE International Conference on*, May 2009, pp. 2098–2105.

[19] N. Chen, K. P. Tee, and C.-M. Chew, "Teleoperation grasp assistance using infra-red sensor array," *Robotica*, vol. 33, no. 04, pp. 986–1002, 2015.

[20] S. Ye, K. Suzuki, Y. Suzuki, M. Ishikawa, and M. Shimojo, "Robust robotic grasping using IR net-structure proximity sensor to handle objects with unknown position and attitude," in *Robotics and Automation (ICRA), 2013 IEEE International Conference on*, May 2013, pp. 3271–3278.

[21] "Asus xtion pro live home page," online; accessed 22-February-2016. [Online]. Available: https://www.asus.com/3D-Sensor/Xtion_PRO_LIVE/

[22] R. Bischoff, J. Kurth, G. Schreiber, R. Koeppe, A. Albu-Schffer, A. Beyer, O. Eiberger, S. Haddadin, A. Stemmer, G. Grunwald, and G. Hirzinger, "The kuka-dlr lightweight robot arm - a new reference platform for robotics research and manufacturing," in *Robotics (ISR), 2010 41st International Symposium on and 2010 6th German Conference on Robotics (ROBOTIK)*. IEEE, 2010.

[23] “Hdsl9100 datasheet page,” online; accessed 18-February-2016. [Online]. Available: http://www.avagotech.com/docs/AV02-2259EN